Design, Simulation, Fabrication and Analysis of Imbalanced Mach Zehnder Interferometers

Pari[1]

[1]Affiliation not available

April 14, 2025

Abstract

Abstract- The goal of this proposal is to review the design and simulations of various Mach Zehnder Interferometers to determine the interference effect of a path length difference ΔL on free spectral range. This is done by simulating the designs using MODE and INTERCONNECT applications.

1 Introduction

Silicon Photonics is an important part of the future of AI applications and high performance compute. As the limitations of electrical interconnects approach, silicon photonics opens up the way to optimizing power efficiency and capacity of data centers along with speeding up data communication. There are many components that build up a photonics integrated circuit used to create fast and efficient transceivers. One of the key components includes a Mach Zehnder Interferometer, which is what this proposal explores.

2 Theory

The Mach Zehnder Interferometer is a device built up of one input that splits the light 50/50 into two outputs generally using a directional coupler or Y-splitter. The split signal goes through two arms, then recombines using another directional coupler or Y-combiner. By adding a path length difference in one arm, as shown in the Fig 1, a phase shift is created between the two signals. This phase shift creates an interference pattern based on constructive or destructive interference when the signals are recombined.

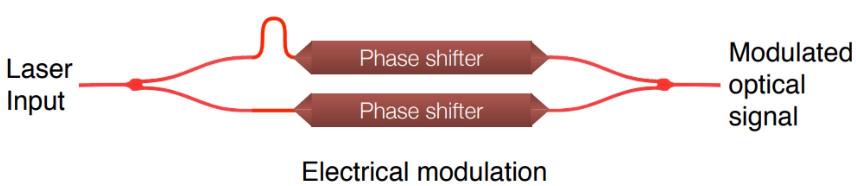

Figure 1: Imbalanced Mach Zehnder Interferometer (will draw my own for the final report

Let's look at the equations for characterizing this imbalanced Mach Zehnder Interferometer. Firstly, we must consider a compact model equation to characterize the waveguide. We use the 2nd order Taylor polynomial function to parameterize the waveguide model for effective index vs. wavelength: $neff(\lambda) =$

$n1 + n2 \cdot (\lambda - \lambda 0) + n3 \cdot (\lambda - \lambda 0)^2$. Using this, we can create a compact model for the waveguide to use in the full circuit simulation of the MZI.

We, then, consider the transfer function for an imbalanced MZI when the waveguides are identical:

$$\frac{Io}{Ii} = \frac{1}{2}\left[1 + \cos\left(\beta \cdot DL\right)\right]$$

where $\beta = \frac{2\pi n}{\lambda}$, FSR = [?]λ = λm+1 - λm = $\frac{\lambda^2}{DL \cdot ng}$, $ng = n - \lambda \cdot \frac{dn}{d\lambda}$)

We can use this to determine the path length difference needed based on the intensity we want transmitted along with the FSR of the MZI.

3 Modelling and Simulation

In this proposal, we would like to design various MZI's with varying path lengths to validate our calculations for the effect on free spectral range. Additionally, we will create circuits to compare the effects of using a Y-splitter/combiner vs. a directional coupler in an MZI.

First, we create the waveguide and run an FDE simulation to get the effective index vs wavelength and group index vs wavelength curves. We use Lumerical MODE in order to run these simulations.

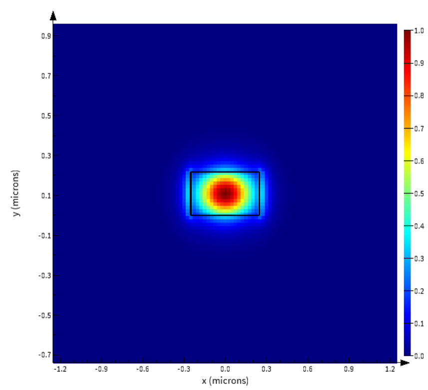

Figure 2: TE Mode profile of 500nm by 220nm waveguide

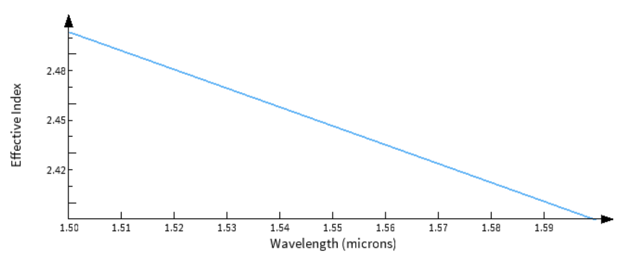

Figure 3: Effective Index of 500nm by 220nm waveguide

From this, we can run our script to get the data from the simulation and calculate the compact model parameters in the Taylor expansion. We get n1 = 2.44682, n2 = -1.3339, and n3 = -0.0439366.

We can now use this compact model to simulate our different MZI designs in Lumerical INTERCONNECT. Since we are utilizing KLayout to set up the GDS file for fabrication, we can also create the designs there and

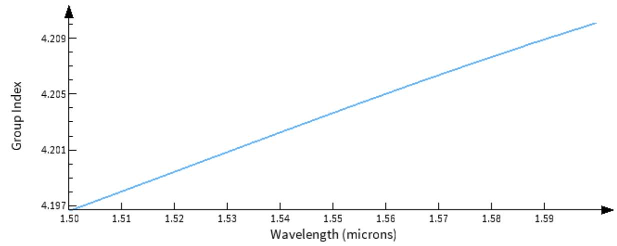

Figure 4: Group Index of 500nm by 220nm waveguide

then run simulations on INTERCONNECT. The design consists of a set of three MZI's with varying path differences of 50um, 100um, and 135um. Below are the simulation results comparing the three designs gain spectrum and FSR, along with the results from the grating coupler to grating coupler reference structure.

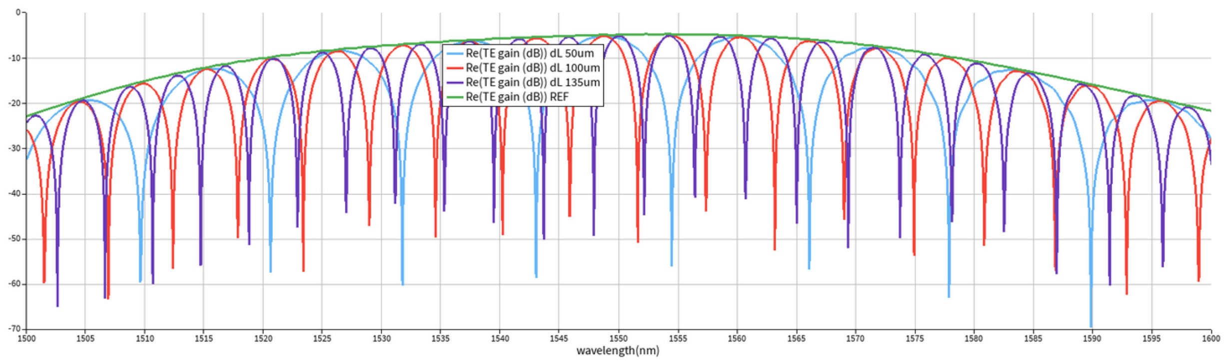

Figure 5: MZI Gain spectrum wavelength [nm] vs gain [dB] showing comparison of delta L = 50um, 100um, 135um

As we can see in the graph, the spectrums match the GC to GC reference structure curve, which confirms the insertion loss is coming from the grating couplers. We can also see that as the path difference gets larger, the FSR gets smaller which aligns with the equations.

In addition to these MZI's presented with results, the layout also contains some other types of MZI's and a Bragg grating structure, which I will cover further in the final paper.

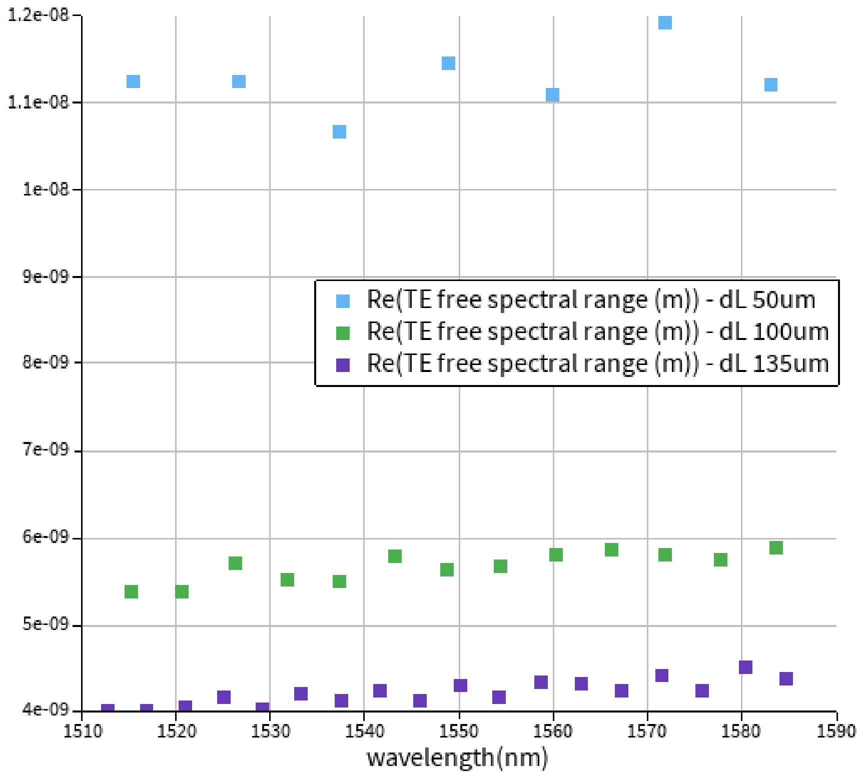

Figure 6: FSR comparison of delta L = 50um, 100um, 135um

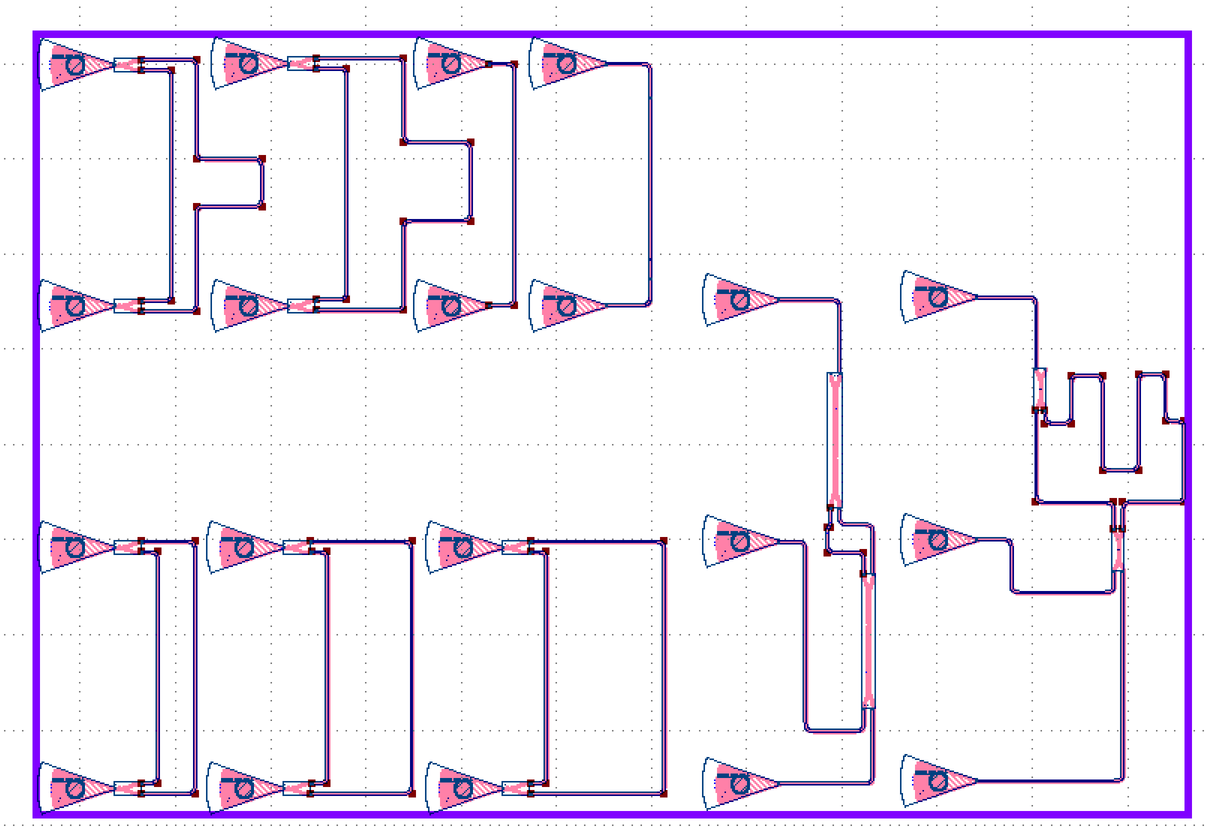

Figure 7: Overview of KLayout Structures

4

5 Fabrication

5.1 Washington Nanofabrication Facility (WNF) silicon photonics process

The devices were fabricated using 100 keV Electron Beam Lithography [1]. The fabrication used silicon-on-insulator wafer with 220 nm thick silicon on 3 µm thick silicon dioxide. The substrates were 25 mm squares diced from 150 mm wafers. After a solvent rinse and hot-plate dehydration bake, hydrogen silsesquioxane resist (HSQ, Dow-Corning XP-1541-006) was spin-coated at 4000 rpm, then hotplate baked at 80 °C for 4 minutes. Electron beam lithography was performed using a JEOL JBX-6300FS system operated at 100 keV energy, 8 nA beam current, and 500 µm exposure field size. The machine grid used for shape placement was 1 nm, while the beam stepping grid, the spacing between dwell points during the shape writing, was 6 nm. An exposure dose of 2800 µC/cm2 was used. The resist was developed by immersion in 25% tetramethylammonium hydroxide for 4 minutes, followed by a flowing deionized water rinse for 60 s, an isopropanol rinse for 10 s, and then blown dry with nitrogen. The silicon was removed from unexposed areas using inductively coupled plasma etching in an Oxford Plasmalab System 100, with a chlorine gas flow of 20 sccm, pressure of 12 mT, ICP power of 800 W, bias power of 40 W, and a platen temperature of 20 °C, resulting in a bias voltage of 185 V. During etching, chips were mounted on a 100 mm silicon carrier wafer using perfluoropolyether vacuum oil. Cladding oxide was deposited using plasma enhanced chemical vapor deposition (PECVD) in an Oxford Plasmalab System 100 with a silane (SiH4) flow of 13.0 sccm, nitrous oxide (N2O) flow of 1000.0 sccm, high-purity nitrogen (N2) flow of 500.0 sccm, pressure at 1400mT, high-frequency RF power of 120W, and a platen temperature of 350C. During deposition, chips rest directly on a silicon carrier wafer and are buffered by silicon pieces on all sides to aid uniformity.(*Course — EdX*)

5.2 Measurement description:

To characterize the devices, a custom-built automated test setup [2, 6] with automated control software written in Python was used [3]. An Agilent 81600B tunable laser was used as the input source and Agilent 81635A optical power sensors as the output detectors. The wavelength was swept from 1500 to 1600 nm in 10 pm steps. A polarization maintaining (PM) fibre was used to maintain the polarization state of the light, to couple the TE polarization into the grating couplers [4]. A 90º rotation was used to inject light into the TM grating couplers [4]. A polarization maintaining fibre array was used to couple light in/out of the chip [5].(*Course — EdX*)

6 Experimental Data

Once the devices were characterized by the automated test setup, I plotted the data using Matlab Online. Figure 8 above shows the collected experimental data for the 100um length difference MZI structure and the reference structure. Figure 9 shows the curve baseline corrected and peaks found for FSR and ng calculations and Figure 10 and 11 show the calculated group index and FSR over wavelength of the measured structure. Figure 12 below shows a plot comparing the measured data of the 100um length difference vs 135um length difference structures. As we can see, it matches the expected results where 135um would have a smaller spacing. *The graphs are shown for only the MZI structure with a length delta of 100um but the calculations were done for each of the structures.

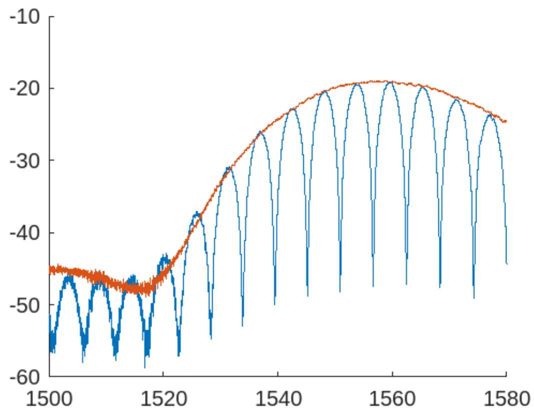

Figure 8: MZI 100um Delta L + REF

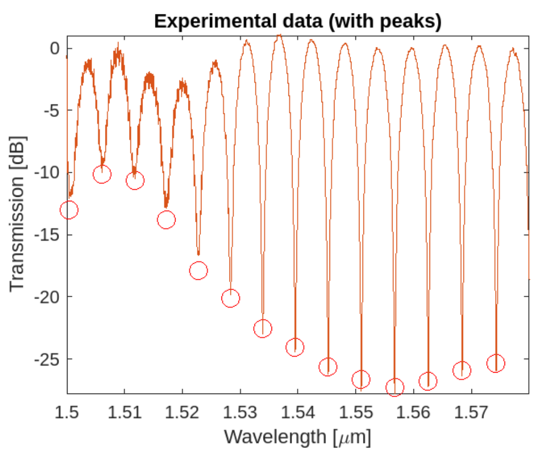

Figure 9: MZI 100um Delta L Baseline Corrected

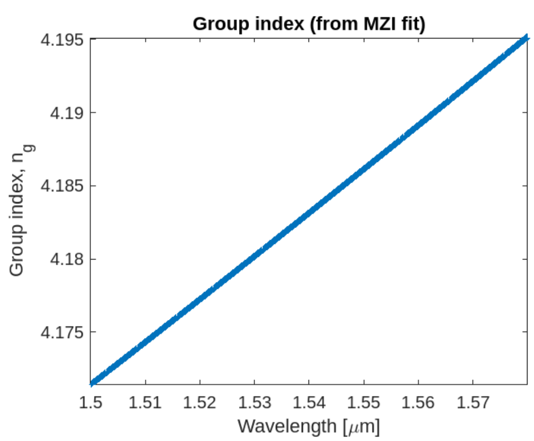

Figure 10: Group Index Experimental

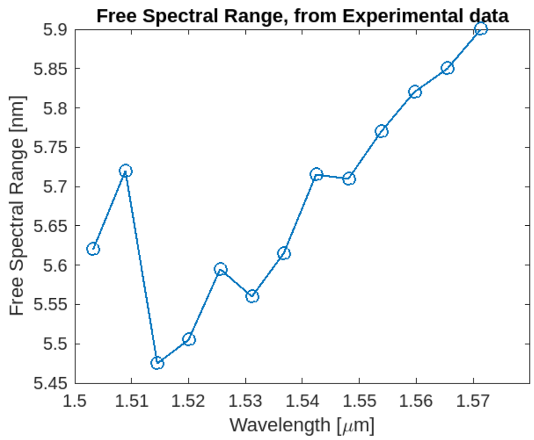

Figure 11: FSR Experimental

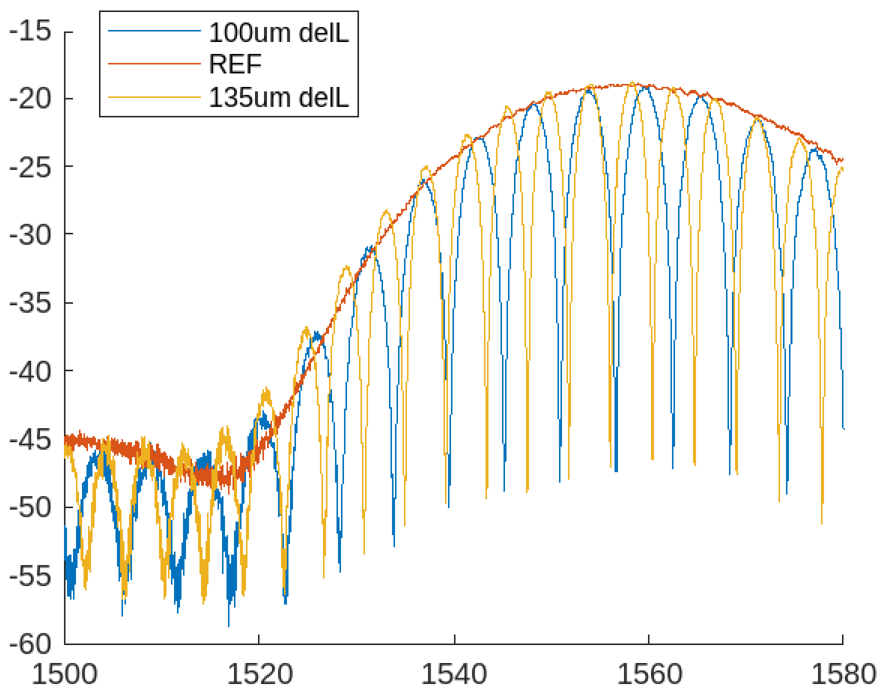

Figure 12: 100um vs 135um and REF

7 Analysis

First, I ran a corner analysis on the 500 by 220nm waveguide to confirm the group index values extracted from the data fit within the range expected. The graphs below show the four corners and the nominal curve for the effective index and group index using the Lumerical EME solver.

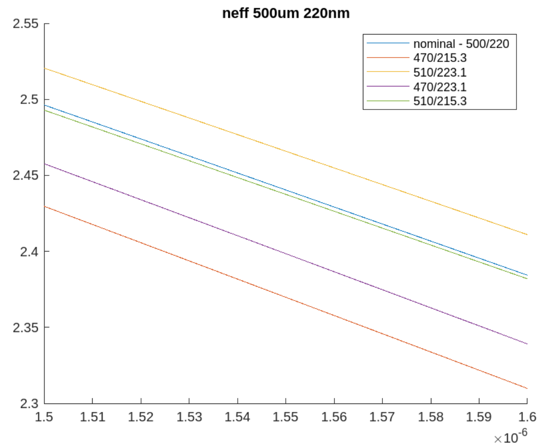

Figure 13: Effective Index Corner Analysis

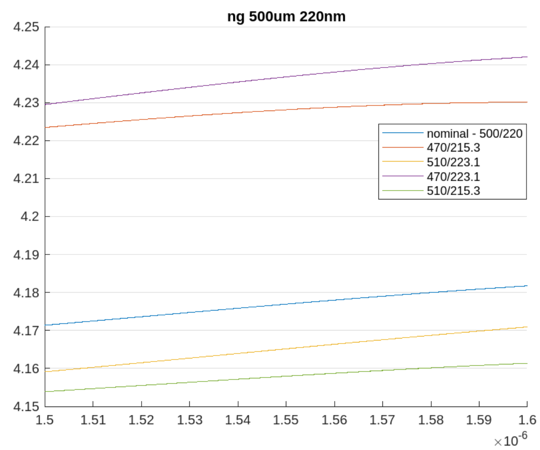

Figure 14: Group Index Corner Analysis

After this, I review the data collected by the automated tool in order to compare results with my expected values from my simulations. As previously mentioned, Figure 9 shows the peaks found for FSR calculation. Using a Matlab script, we calculate the FSR and group index values from the experimental data. Below is a table that shows the comparison between the simulation results and experimental results for two structures to show how accurately we designed the MZI's.

Structure	Simulated FSR	Simulated ng	Experimental FSR	Experimental ng
MZI 100um delL	5.656	4.176	5.71	4.159
MZI 135um delL	4.292	4.176	4.265	4.1813

We see that it is not exactly the simulated value because of fabrication and manufacturing variabilities, which is why we run the corner analysis to account for this. The group index values accurately fits within the expected range we found from the corner analysis. This confirmed that the layout was correctly made in KLayout and the simulations were accurately done in order to create the structures I wanted.

8 Conclusion

In conclusion, we can see that our simulations were run successfully to correctly fabricate various structures. This report clearly describes all the steps taken from using equations to understand the theory, to simulating the waveguide using Lumerical and creating compact models, to laying out the structures in KLayout and having them fabricated and measured. The results from the experimental data confirm that the fabrication process was also successful and we correctly normalize the data and find the FSR and group index to match the simulated results.

9 Acknowledgements

I/We acknowledge the edX UBCx Phot1x Silicon Photonics Design, Fabrication and Data Analysis course, which is supported by the Natural Sciences and Engineering Research Council of Canada (NSERC) Silicon Electronic-Photonic Integrated Circuits (SiEPIC) Program. The devices were fabricated by Richard Bojko at the University of Washington Washington Nanofabrication Facility, part of the National Science Foundation's National Nanotechnology Infrastructure Network (NNIN), and Cameron Horvath at Applied Nanotools, Inc. Omid Esmaeeli performed the measurements at The University of British Columbia. We acknowledge Lumerical Solutions, Inc., Mathworks, Mentor Graphics, Python, and KLayout for the design software. (*Course — EdX*)

10 References

[1] edX UBC Phot1x: Silicon Photonics Design, Fabrication and Data Analysis

[2] Lukas Chrostowski, Michael Hochberg, "Silicon Photonics Design: From Devices to Systems", Cambridge University Press, 2015

[3] `http://siepic.ubc.ca/probestation`, using Python code developed by Michael Caverley.

[4] Tools: KLayout, Lumerical Interconnect, Lumerical MODE

[5] R. J. Bojko, J. Li, L. He, T. Baehr-Jones, M. Hochberg, and Y. Aida, "Electron beam lithography writing strategies for low loss, high confinement silicon optical waveguides," J. Vacuum Sci. Technol. B 29, 06F309 (2011)

References

https://learning.edx.org/course/course-v1:UBCx+Phot1x+1T2025/block-v1:UBCx+Phot1x+1T2025+type@sequential+block@de8ebefd6784432588063f67eb3b6ce9/block-v1:UBCx+Phot1x+1T2025+type@vertical+block@b2ebecff9e4b4d2f9e3f9f7bc153384e, https://learning.edx.org/course/course-v1:UBCx+Phot1x+1T2025/block-v1:UBCx+Phot1x+1T2025+type@sequential+block@de8ebefd6784432588063f67eb3b6ce9/block-v1:UBCx+Phot1x+1T2025+type@vertical+block@b2ebecff9e4b4d2f9e3f9f7bc153384e.